Computer Vision Technology for X-ray Testing

Domingo Mery
Department of Computer Science
Pontificia Universidad Católica de Chile

Av. Vicuña Mackenna 4860(143) – Santiago de Chile
dmery@ing.puc.cl http://dmery.ing.puc.cl

Abstract

X-ray testing has been developed for inspection of materials or objects, where the aim is to analyze –nondestructively– those inner parts that are undetectable to the naked eye. Thus, X-ray testing is used to determine if a test object deviates from a given set of specifications. Typical applications are inspection of automotive parts, quality control of welds, screening of baggage, analysis of food products and inspection of cargos. In order to achieve efficient and effective X-ray testing, automated and semi-automated systems based on computer vision algorithms are being developed to execute this task. In this paper, we present a general overview of computer vision approaches that have been used in X-ray testing. In addition, we review some techniques that have been applied in certain relevant applications; and we introduce a public database of X-ray images that can be used for testing and evaluation of image analysis and computer vision algorithms. Finally, we conclude that there are some areas –like casting inspection where automated systems are very effective, and other application areas – such as baggage screening– where human inspection is still used; there are certain application areas –like weld and cargo inspections– where the process is semi-automatic; and there is some research in areas –including food analysis– where processes are beginning to be characterized by the use of X-ray imaging.

1 Introduction

X-ray testing is used in many applications such as: analysis of food products, screening of baggage, inspection of automotive parts, and quality control of welds, among others. X-ray testing usually involves measurement of specific part features such as integrity or geometric dimensions in order to detect, recognize or evaluate wanted (or unwanted) inner parts. Automated and semi-automated systems are being developed to execute this difficult, tedious and –sometimes– dangerous task. Compared to manual X-ray testing, automated systems offer the advantages of objectivity and reproducibility for every test. Fundamental disadvantages are, however, the complexity of their configuration, the inflexibility to any change in the evaluation process, and

sometimes the inability to analyze intricate images, which is something that people can generally do well. Research and development is, however, ongoing into automated adaptive processes to accommodate modifications.

In this paper, we present the state of the art in X-ray testing using computer vision. We describe a general overview of computer vision methodologies that have been used over the last few years (Section 2). In addition, we review some techniques that have been applied in certain relevant applications using X-ray testing (Section 3). Finally, we introduce a public database of X-ray images that can be used for testing and evaluation of image analysis and computer vision algorithms (Section 4). The paper ends with relevant concluding remarks (Section 5). A previous version of this paper was presented in [38, 39].

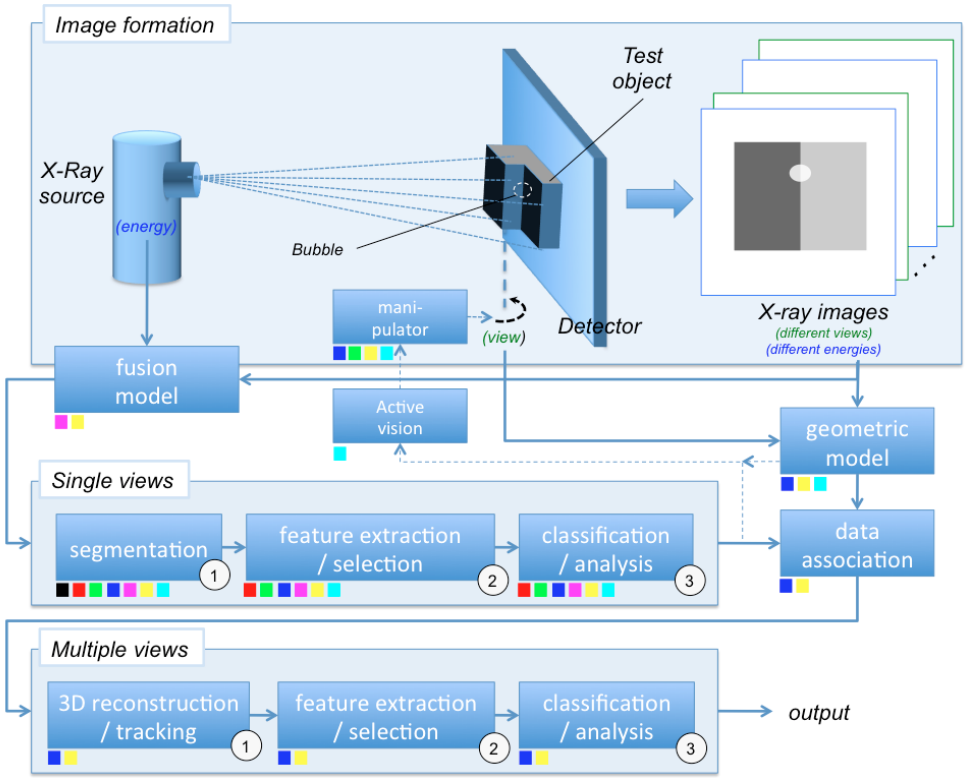

Figure 1: General schema for X-ray testing using computer vision. X-ray images of a test object can be generated at different positions and different energy levels. Depending on the application, each block of this diagram can be (or not be) used. For example, there are applications such as weld inspection that use a segmentation of a single mono energetic X-ray image (black square), sometimes with pattern recognition approaches (red squares); applications like casting inspection that use mono energetic multiple views where the decision is taken analyzing individual views (green squares) or corresponding multiple views (blue squares); applications including baggage screening that use dual-energy of single views (magenta squares) and multiple views (yellow squares); and finally, applications on cargo

inspection that employ active vision where a next best view is set according to the information of a single view (cyan squares). In each case, the blocks without the corresponding color square are not used.

2 Principles

In this Section, the principles that govern the X-ray testing by computer vision are presented as a general model according to Fig. 1. Applications on X-ray testing –as will be seen in next Section– follow this general schema. Depending on the way the X-ray images are acquired and analyzed, each block can be (or can be not) used. For instance, in baggage inspection there are methods that analyze single or multiple views, using mono-energetic or dual-energy systems. For each one of these four combinations, only the corresponding blocks of Fig. 1 are to be used as illustrated with the color squares.

This Section covers *i)* X-ray image formation, *ii)* single view analysis, *iii)* geometric model and *iv)* multiple view analysis.

2.1 X-ray image formation

X-ray testing is a form of non-destructive testing (NDT) defined as a task that uses X-ray imaging to determine if a test object deviates from a given set of specifications, without changing or altering that object in any way [22]. In X-ray testing, X-ray radiation is passed through the test object, and a detector captures an X-ray image corresponding to the radiation intensity attenuated by the object [1]. According to the principle of photoelectric absorption [3]:

$$I = I_0 \exp(-\mu z) \tag{1}$$

the transmitted intensity I depends on the incident radiation intensity I_0, the thickness z of the test object, and the energy dependent linear attenuation coefficient μ associated with the material, as illustrated in Fig. 2.

[1] X-rays can be absorbed or scattered by the test object. In this paper we will cover only the first interaction. For an interesting application based on the X-ray scattering effect, the reader is referred to [68].

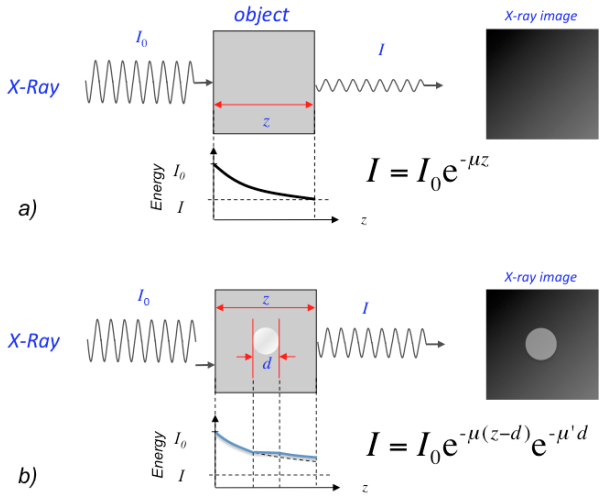

Figure 2: X-ray image formation according to absorption law: a) X-ray image of a homogenous object, and b) X-ray image of an object with two different materials.

The most widely used X-ray imaging systems employed in X-ray testing are digital radiography (DR) and computed tomography (CT) imaging[2]. On the one hand, DR emphasizes high throughput. It uses electronic sensors (instead of traditional radiographic film) to obtain a digital X-ray projection of the target object, for this reason it is simple and quick. A flat amorphous silicon detector can be used as an image sensor in X-ray testing systems. In such detectors, and using a semi-conductor, energy from the X-ray is converted directly into an electrical signal that can be digitalized into an X-ray digital image [53]. On the other hand, CT imaging provides a cross-section image of the target object so that each object is clearly separated from each other, however, CT imaging requires a considerable number of projections to reconstruct an accurate cross-section image, which is time consuming.

It is worth noting that if X-ray radiation passes through n different materials, with attenuation coefficients μ_i and thickness z_i , for $i = 1, \ldots n$, the transmitted intensity I can be expressed as

$$I = I_0 \exp(-\textstyle\sum_i \mu_i z_i). \qquad (2)$$

This explains the image generation of regions that are present inside the test object, as shown in Fig. 2, where a gas bubble is clearly detectable. Nevertheless, X-ray images sometimes contain overlapped objects, making it extremely difficult to distinguish them properly.

[2] Computed tomography is beyond the scope of this paper. For NDT applications using CT, the reader is referred to [16].

Coefficient μ in (1) can be modeled as $\mu = \alpha(Z,E)\rho$, where ρ is the density of the material, and $\alpha(Z,E)$ is the mass attenuation coefficient that depends on the atomic number of the material Z, and the energy E of the X-ray photons. Values for $\alpha(Z,E)$ are already measured and available in several tables (see [23]). In order to identify the material composition –typically for explosives or drug detection– the atomic number Z cannot be estimated using only one image, as a thin material with a high atomic number can have the same absorption as a thick material with a low atomic number [68]. For this purpose, a dual-energy system is used, where the object is irradiated with a high energy level E_1 and a low level energy E_2. In the first case, the absorbed energy depends mainly on the density of the material. In the second case, however, the absorbed energy depends primarily on the effective atomic number and the thickness of the material [59]. Using dual-energy, it is possible to calculate the ratio $R = \ln(I_2/I_0) \ / \ \ln(I_1/I_0)$, where I_1 and I_2 are the transmitted intensities I obtained by (1) using energies E_1 and E_2 respectively. Thus, from $R = \alpha(Z,E_2)/\ \alpha(Z,E_1)$, the term $-\rho z$ is canceled out, Z can be directly found using the known measurements $\alpha(Z,E)$ [21]. From both images, a new image is generated using a fusion model, usually a look-up-table that produces pseudo color information [14, 5], as shown in Fig. 3.

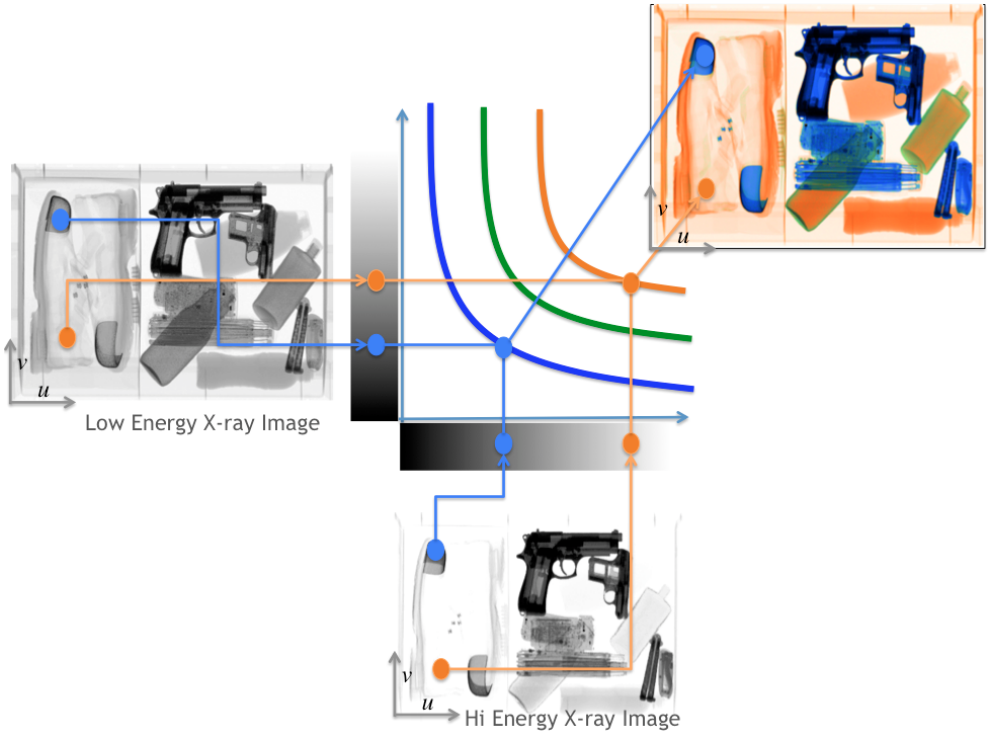

Figure 3: Generation of a pseudo-color image using dual-energy. In this example orange is for organic materials, and blue is for metals. The intensity of this image corresponds to the thickness of the materials.

2.2 Single view analysis

A computer vision system for single view analysis, as shown in Fig. 1, consists typically of the following steps: an X-ray image of the test object is taken and stored in a computer. The digital image is improved in order to enhance the details. The X-ray image of the parts of interest is found and isolated from the background of the scene. Significant features of the segmented parts are extracted. Selected features are classified or analyzed in order to determine if the test object deviates from a given set of specifications. Using a supervised pattern recognition methodology, the selection of the features and the training of the classifier are performed using representative images that are to be labeled by experts [12].

For the segmentation task, two general approaches can be used: a traditional image segmentation or a sliding–window approach. In the first case, image processing algorithms are used (*e.g.*, histograms, edge detection, morphological operations, filtering, etc. [17]). Nevertheless, inherent limitations of traditional segmentation algorithms for complex tasks and increasing computational power have fostered the emergence of an alternative approach based on the so-called sliding–window paradigm. Sliding–window approaches have established themselves as state–of–art in computer vision problems where a visually complex object must be separated from the background (see, for example, successful applications in face detection [65] and human detection [9]). In the sliding–window approach, a detection window is moved over an input image in both horizontal and vertical directions, and for each localization of the detection window, a classifier decides to which class the corresponding portion of the image belongs according to its features. Here, a set of candidate image areas are selected and all of them are fed to the subsequent parts of the image analysis algorithm. This resembles a brute force approach where the algorithm explores a large set of possible segmentations, and at the end the most suitable is selected by the classification steps. An example for weld inspection using sliding-windows can be found in [37].

2.3 Geometric model

The X-ray image of a test object corresponds to a projection in perspective, where a 3D point of the test object is viewed as a pixel in the digital X-ray image, as illustrated in Fig. 4. A geometric model that describes this projection can be very useful for 3D reconstruction and for data association between different views of the same object. Thus, 3D features or multiple view 2D features can be used to improve the diagnosis performed by using a single view.

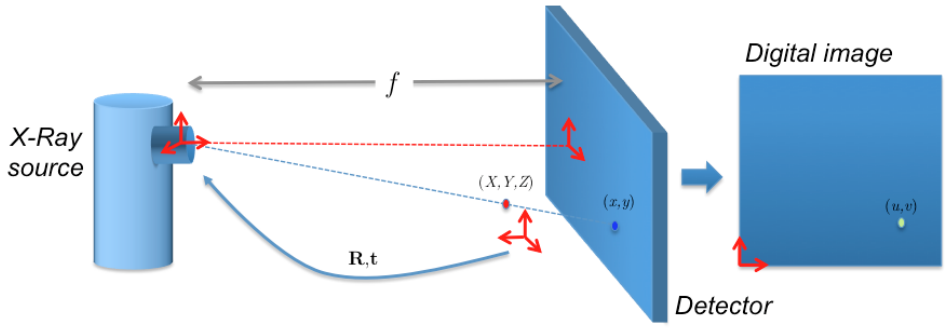

Figure 4: Geometric model: a 3D point (X, Y, Z) is projected as a 2D point (u, v).

For the geometric model, four coordinate systems are used (see Fig. 4):

- OCS (X, Y, Z): Object Coordinate System, where a 3D point is defined using coordinates attached to the test object.

- WCS (X ', Y ', Z '): World Coordinate System, where the origin corresponds to the optical center (X-ray source) and the Z ' axis is perpendicular to the projection plane of the detector.

- PCS (x, y): Projection Coordinate System, where the 3D point is projected into projection plane Z ' = f, and the origin is the intersection of this plane with Z 'axis.

- ICS (u, v): Image Coordinate System, where a projected point is viewed in the image. In this case, (x, y)–axes are set to be parallel to (u, v)–axes.

The geometric model OCS → ICS, i.e., transformation **P**: (X, Y, Z) → (u, v), can be expressed in homogeneous coordinates as [33]:

$$\lambda \begin{bmatrix} u \\ v \\ 1 \end{bmatrix} = \mathbf{P} \begin{bmatrix} X \\ Y \\ Z \\ 1 \end{bmatrix} \tag{3}$$

where λ is a scale factor and P is a 3 × 4 matrix modeled as three transformations:

i) OCS → WCS, i.e., transformation $\mathbf{T}_1$: $(X, Y, Z) \rightarrow (X', Y', Z')$, using a 3D rotation matrix **R**, and 3D translation vector **t**;

ii) WCS → (PCS), i.e., transformation $\mathbf{T}_2$: $(X', Y', Z') \rightarrow (x, y)$, using a perspective projection matrix that depends on focal distance f; and

iii) PCS → ICS, i.e., transformation $\mathbf{T}_3$: $(x, y) \rightarrow (u, v)$, using scales factor α_x and α_y , and 2D translation vector (u_0, v_0).

The three transformations OCS → WCS → PCS → ICS are expressed as:

$$\mathbf{P} = \underbrace{\begin{bmatrix} \alpha_x & 0 & u_0 \\ 0 & \alpha_y & v_0 \\ 0 & 0 & 1 \end{bmatrix}}_{\mathbf{T}_3} \underbrace{\begin{bmatrix} f & 0 & 0 & 0 \\ 0 & f & 0 & 0 \\ 0 & 0 & 1 & 0 \end{bmatrix}}_{\mathbf{T}_2} \underbrace{\begin{bmatrix} \mathbf{R} & \mathbf{t} \\ \mathbf{0}^{\mathrm{T}} & 1 \end{bmatrix}}_{\mathbf{T}_1} \tag{4}$$

The parameters included in matrix P can be estimated using a calibration approach as illustrated in Fig. 5 [20].

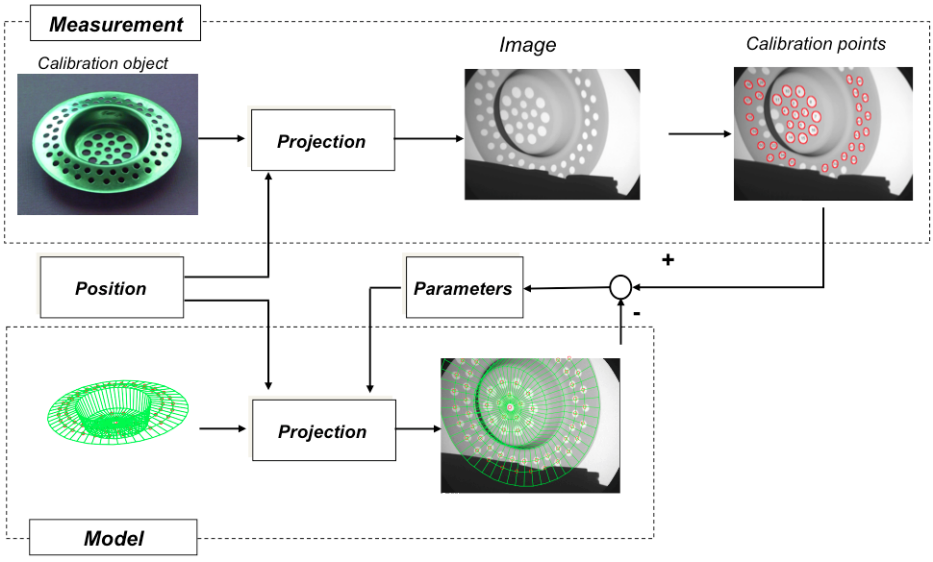

Figure 5: Geometric calibration of a computer vision X-ray imaging system: the modeled projection of a 3D model coincides with real geometry of the calibration object.

In order to obtain multiple views of the object, m different projections of the test object can be achieved by rotating and translating it (for this task a manipulator can be used as shown in Fig. 6). For the k-th projection, for $k = 1, \ldots m$, the geometric model $\mathbf{P}_k$ used in (3) is computed from (4) including 3D rotation matrix $\mathbf{R}_k$ and 3D translation $\mathbf{t}_k$. Matrices $\mathbf{P}_k$ can be estimated using a calibration object projected in the m different positions [33] or using a bundle adjustment algorithm where the geometric model is obtained from the m X-ray images of the test object [36].

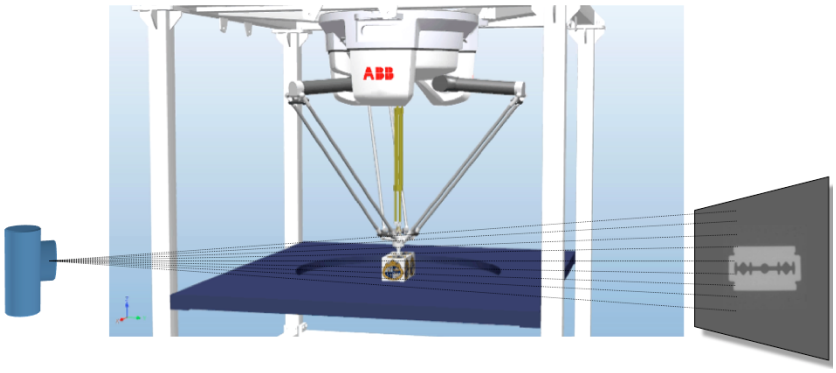

Figure 6: Generally a manipulator is used to locate the test object in a desired position.

2.4 Multiple view analysis

It is well known that an image says more than thousand words, however, this is not always true if we have an intricate image. In certain X-ray applications, *e.g.*, baggage inspection, there are usually intricate X-ray images due to overlapping parts inside the test object, where each pixel corresponds to the attenuation of multiple parts, as expressed in (2).

In some cases, active vision can be used in order to adequate the viewpoint of the test object to obtain more suitable X-ray images to analyze. Therefore, an algorithm is designed for guiding the manipulator of the X-ray imaging system to poses where the detection performance should be higher [52] (see Fig. 1).

In other cases, multiple view analysis can be a powerful option for examining complex objects where uncertainty can lead to misinterpretation. Multiple view analysis offers advantages not only in 3D interpretation. Two or more views of the same object taken from different viewpoints can be used to confirm and improve the diagnostic done by analyzing only one image. In the computer vision community, there are many important contributions in multiple view analysis (*e.g.*, object class detection [60], motion segmentation [72], simultaneous localization and mapping (SLAM) [25], 3D reconstruction [2], people tracking [13], breast cancer detection [62] and quality control [7]). In these fields, the use of multiple view information yields a significant improvement in performance.

Multiple view analysis in X-ray testing can be used to achieve two main goals: *i)* analysis of 2D corresponding features across the multiple views, and *ii)* analysis of 3D features obtained from a 3D reconstruction approach. In both cases, the attempt is made to gain relevant information about the test object. For instance, in order to validate a single view detection –filtering out false alarms– 2D corresponding features can be analyzed [41]. On the other hand, if the geometric dimension of an inner part must be measured a 3D reconstruction must be performed [47].

As illustrated in Fig. 1, the input of the multiple view analysis is the associated data, i.e., corresponding points (or patches) across the multiple views. To this end, associated 2D cues are found using geometric constraints (*e.g.*, epipolar geometry and multifocal tensors [20, 34]), and local scale-invariant descriptors across multiple views (*e.g.*, like SIFT [30]).

Finally, 2D or 3D features of the associated data can be extracted and selected, and a classifier can be trained using the same pattern recognition methodology explained in Section 2.2.

Depending on the application, the output could be a measurement (*e.g.*, the volume of the inspected inner part is 3.4cm^3), a class (*e.g.*, the test object is defective) or an interpretation (*e.g.*, the baggage should be inspected by a human operator because the uncertainty is high).

3 Applications

In this Section, the state of the art of certain relevant applications on X-ray testing will be described. This section covers X-ray testing in *i)* casting, ii) weld, *iii)* baggage, *iv)* food, and *v)* cargo. In Tables 1–5, approaches in each application are summarized showing how they use the different steps of general diagram according to Fig. 1.

Table 1: Castings

Reference	Energy		Geometric	Single Views(**)			Active	Multiple Views(**)		
	Mono	Dual	Model(*)	(1)	(2)	(3)	Vision	(1)	(2)	(3)
Carrasco (2011) [6]	×		N	×	×	×	–	×	×	×
Li (2006) [27]	×		–	×	×	–	–	–	–	–
Mery (2002) [41]	×		C	×	×	×	–	×	×	×
Mery (2011) [36]	×		N	×	×	×	–	×	×	×
Pieringer (2010) [49]	×		C	×	×	×	–	×	×	×
Pizarro (2008) [50]	×		N	×	×	×	–	×	×	×
Tang (2009) [61]	×		–	×	–	–	–	–	–	–

(*) C: Calibrated, N: Not calibrated, –: not used. (**) See (1), (2), (3) in Fig. 1

3.1 Casting

Light-alloy castings produced for the automotive industry, such as wheel rims, steering knuckles and steering gear boxes are considered important components for overall roadworthiness. Non-homogeneous regions can be formed within the work piece in the production process. These are manifested, for example, by bubble-shaped voids, fractures, inclusions or slag formation. To ensure the safety of construction, it is necessary to check every part thoroughly using X-ray testing. In casting inspection, automated X-ray systems have not only raised quality, through repeated objective inspections and improved processes, but have also increased productivity and consistency by reducing labor costs. An example is illustrated in Fig. 7. A survey can be found in [35]. Selected approaches are summarized in Table 1. In this area, we conclude that automated systems are very effective, because inspection task is fast and achieves high performance.

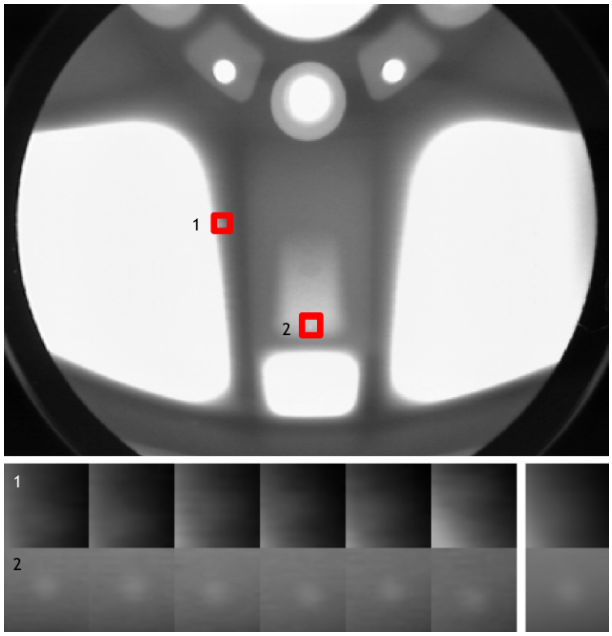

Figure 7: Detection of very smalls flaws in an aluminum wheel using multiple views [36].

3.2 Weld

In welding process, a mandatory inspection using X-ray testing is required in order to detect defects like porosity, inclusion, lack of fusion, lack of penetration and cracks. Industrial X-ray images of welds are widely used for the detecting those defects in the petroleum, chemical, nuclear, naval, aeronautics and civil construction industries, among others. An example is illustrated in Fig. 8. A survey can be found in [56, 57]. Selected approaches are summarized in Table 2. As we can see there is much research on weld inspection. Achieved performance of the developed algorithms is still not high enough, hence it is not suitable for fully automated inspection.

Table 2: Welds

Reference	Energy		Geometric	Single Views(**)			Active	Multiple Views(**)		
	Mono	Dual	Model(*)	(1)	(2)	(3)	Vision	(1)	(2)	(3)
Liao (2008) [28]	×		–	×	×	×	–	–	–	–
Liao (2009) [29]	×		–	×	×	×	–	–	–	–
Mery (2003) [40]	×		–	×	×	×	–	–	–	–
Mery (2011) [37]	×		–	×	×	×	–	–	–	–
Vilar (2009) [64]	×		–	×	×	×	–	–	–	–
Wang (2008) [67]	×		–	×	×	×	–	–	–	–
Shi (2007) [55]	×		–	×	×	×	–	–	–	–

(*) C: Calibrated, N: Not calibrated, –: not used. (**) See (1), (2), (3) in Fig. 1

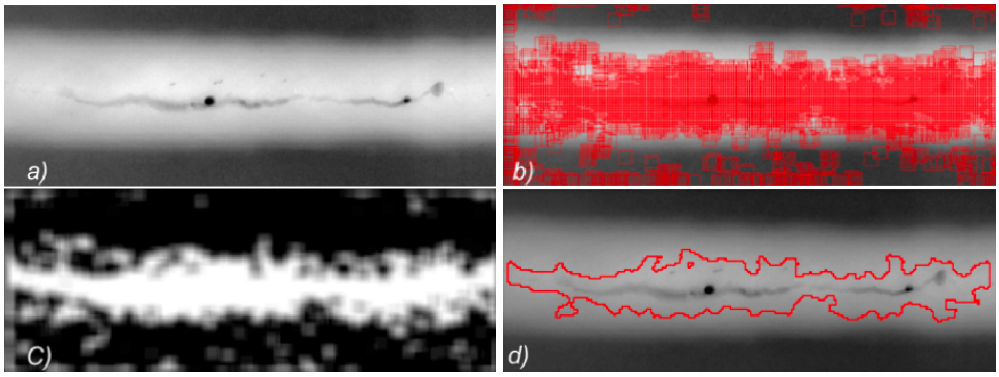

Figure 8: Weld inspection using a sliding-window: a) X-ray image, b) detected windows, c) activation map, d) detection [37].

3.3 Baggage

Since 11/9, automated (or semi-automated) 3D recognition using X-ray images has become a very important issue in baggage screening [69, 46]. The inspection process is very complex because threat items are very difficult to detect when placed in close packed bags, superimposed by other objects, and/or rotated showing an unrecognizable view. During the last decade, however, relevant research has been done in multiple view analysis and dual-energy imaging. The use of multiple view information yields a significant improvement in performance because certain items are difficult to be recognized using only one viewpoint [66].

Table 3: Baggage

Reference	Energy		Geometric	Single Views(**)			Active	Multiple Views(**)		
	Mono	Dual	Model(*)	(1)	(2)	(3)	Vision	(1)	(2)	(3)
Abusaeeda (2011) [1]	×	×	C	–	×	–	–	–	×	–
Baştan (2012) [5]	×	×	–	×	×	×	–	–	–	–
Baştan (2013) [4]	×	×	–	×	×	×	–	×	×	×
Chen (2005) [8]	×	×	–	×	×	–	–	–	–	–
Ding (2006) [10]	×	×	–	×	×	×	–	–	–	–
Franzel (2012) [14]	×	×	C	×	×	×	–	×	×	×
Heitz (2010) [21]	×	×	–	×	×	×	–	×	×	×
Mansoor (2012) [32]	×	×	–	×	×	×	–	–	–	–
Mery (2011) [36]	×		N	×	×	×	–	×	×	×
Mery (2013) [43]	×		N	×	×	×	–	×	×	×
Mery (2013) [44]	×		N	×	×	×	–	×	×	×
Qiang (2006) [31]	×	×	–	×	×	–	–	–	–	–
Riffo (2011) [52]	×		N	×	×	–	×	×	×	×
Schmidt (2012) [54]	×	×	–	×	×	×	–	–	–	–
Turcsany (2013) [63]	×	×	–	×	×	×	–	–	–	–

(*) C: Calibrated, N: Not calibrated, –: not used. (**) See (1), (2), (3) in Fig. 1

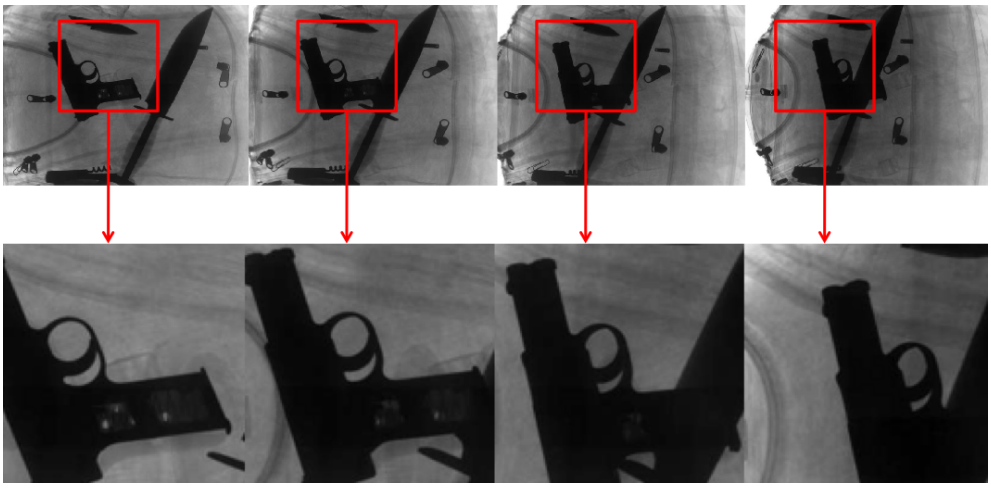

Figure 9: Detection of a guns based on the trigger identification in multiple views [43].

On the other hand, using dual-energy it is possible to identify the material composition –typically for explosives, drugs and organic materials– [59]. An example is illustrated in Fig. 9. A survey on explosives detection can be found in [59, 68]. Selected approaches are summarized in Table 3. We conclude, that in baggage screening, where human security plays an important role and inspection complexity is very high, human inspectors are still used. For intricate conditions, multiple view X-ray inspection using dual-energy is required.

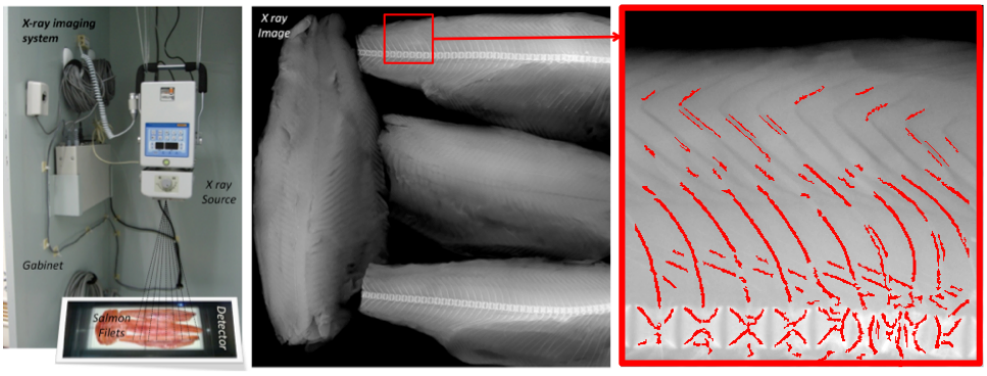

Figure 10: Detection of fish bones using sliding-windows [42].

3.4 Food

In order to ensure food safety inspection, several applications have been developed in food industry. The difficulties inherent in the detection of defects and contaminants in food products have limited the use of X-ray into packaged foods sector. However, the need for NDT has motivated a considerable research effort in this field spanning many decades [19]. The most important advances are: detection of foreign objects in packaged foods [26]; detection of fishbones in fishes [42]; identification of insect infestation in citrus [24]; detection of codling moth larvae in apples [19]; fruit quality inspection like split-pits, water content distribution and internal structure [48]; and detection of larval stages of the granary weevil in wheat kernels [18]. In these applications, only single view analysis is required. An example is illustrated in Fig. 10. A survey can be found in [19]. In Table 4, the mentioned applications are summarized.

Table 4: Food

Reference	Energy		Geometric	Single Views(**)			Active	Multiple Views(**)		
	Mono	Dual	Model(*)	(1)	(2)	(3)	Vision	(1)	(2)	(3)
Haff (2004) [18]	×		–	×	×	×	–	–	–	–
Jiang (2008) [24]	×		–	×	×	×	–	–	–	–
Ogawa (2003) [48]	×		–	×	×	×	–	–	–	–
Kwon (2008) [26]	×		–	×	×	×	–	–	–	–
Mery (2011) [42]	×		–	×	×	×	–	–	–	–

(*) C: Calibrated, N: Not calibrated, –: not used. (**) See (1), (2), (3) in Fig. 1

3.5 Cargo

With the ongoing development of international trade, cargo inspection becomes more and more important. X-ray testing has been used for the evaluation of the contents of cargo, trucks, containers, and passenger vehicles to detect the possible presence of many types of contraband. Some approaches are presented in Table 5. There still is not much research on cargo inspection, and complexity of this inspection task is very high. For this reason, we conclude that these X-ray systems still are semi-automatic only, and they require human supervision.

Table 5: Cargo

Reference	Energy		Geometric	Single Views(**)			Active	Multiple Views(**)		
	Mono	Dual	Model(*)	(1)	(2)	(3)	Vision	(1)	(2)	(3)
Duan (2008) [11]	×		–	×	×	×	–	×	×	–
Frosio (2011) [15]	×		–	×	×	×	×	×	×	–
Zhu (2008) [71]	×		–	×	×	×	–	×	×	–
Zhu (2010) [70]	×		–	×	×	×	–	×	×	–

(*) C: Calibrated, N: Not calibrated, –: not used. (**) See (1), (2), (3) in Fig. 1

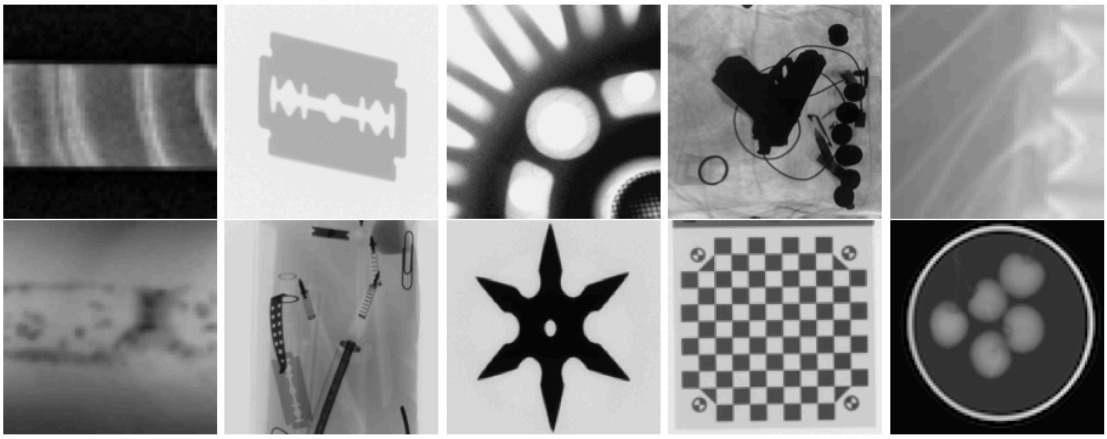

Figure 11: Some X-ray images of our public database GDXray: wood, razor blade, aluminum wheel, bag with a gun, fishbones, weld, pen case, shruriken, calibration pattern and apples.

4 Databases

Public databases of X-ray images can be found for medical imaging[3], however, to the best knowledge of the author of this article, up until now there have not been public databases of digital X-ray images for X-ray testing.

As a service to the X-ray testing community, we collected more than 3.000 X-ray images for the development, testing and evaluation of image analysis and computer vision algorithms. The images are organized in a public database called GDXray: The GRIMA X-ray database[4]. The database includes three groups of X-ray images: metal objects (castings, welds, razor blades, ninja stars (shuriken), guns, knives and sink strainers), baggages (bags and pen cases); and natural objects (fruits, fishbones and wood). Some examples are illustrated in Fig. 7–11.

5 Conclusions

[3] See for example a good collection in http://www.via.cornell.edu/databases/

[4] GRIMA is the name of our Machine Intelligence Group at the Department of Computer Science of the Pontificia Universidad Catóica de Chile http://grima.ing.puc.cl. The X-ray images included in GDXray can be used free of charge, for research and educational purposes only. Redistribution and commercial use is prohibited. Any researcher reporting results which use this database should acknowledge the GDXray database by citing [45].

In this paper we presented a general overview of computer vision methodologies that have been used in X-ray testing, as illustrated in diagram of Fig. 1. The presented applications on X-ray testing follows this general schema, where depending on the way the X-ray images are acquired and analyzed, each step can be (or can be not) used.

In the presented applications, we observe that there are some areas, like casting inspection, where automated systems are very effective; and other application areas, like baggage screening, where human inspection is still used. Additionally, there are certain application areas, like weld and cargo inspection, where the inspection is semi-automatic. Finally, there is some research in food analysis where they are beginning to be characterized using X-ray imaging.

It is clear that many research directions have been exploited, some very different principles have been adopted and a wide variety of algorithms have been developed for very different applications. Nevertheless, automated X-ray testing remains an open question because it still suffers from: *i)* loss of generality because approaches developed for one application may not be used in other one; *ii)* deficient detection accuracy because commonly there is a fundamental trade–off between false alarms and miss detections; *iii)* limited robustness because prerequisites for the use of a method are often fulfilled in simple cases only; and *iv)* low adaptiveness because it may be very difficult to accommodate an automated system to design modifications or different objects.

Compared to manual X-ray testing, automated systems offer advantages of objectivity and reproducibility for every test. Fundamental disadvantages are, however, the complexity of their configuration, the inflexibility to any change in the evaluation process, and sometimes the inability to analyze intricate images, which is something that people can generally do well. Research and development is, however, ongoing into automated adaptive processes to accommodate modifications.

Acknowledgments

This work was supported by grant Fondecyt No. 1130934 from CONICYT–Chile. The author wants to thank M. Bastan from Image Understanding and Pattern Recognition Group, at Technical University of Kaiserslautern, Germany, for sharing pseudo-color image of Fig. 3.

References

[1] O. Abusaeeda, J. Evans, D. D., and J. Chan. View synthesis of KDEX imagery for 3D security X-ray imaging. In Proc. 4th International Conference on Imaging for Crime Detection and Prevention (ICDP-2011), 2011.

[2] S. Agarwal, N. Snavely, I. Simon, S. Seitz, and R. Szeliski. Building Rome in a day. In IEEE 12th International Conference on Computer Vision (ICCV2009), pages 72–79, 2009.

[3] J. Als-Neielsen and D. McMorrow. Elements of modern X-ray physics. Willey, second edition, 2011.

[4] M. Bastan, W. Byeon, and T. M. Breuel. Object Recognition in Multi-View Dual X-ray Images. In British Machine Vision Conference BMVC, 2013.

[5] M. Bastan, M. R. Yousefi, and T. M. Breuel. Visual words on baggage X-ray images. In Computer Analysis of Images and Patterns, pages 360–368. Springer, 2011.

[6] M. Carrasco and D. Mery. Automatic multiple view inspection using geometrical tracking and feature analysis in aluminum wheels. Machine Vision and Applications, 22(1):157–170, 2011.

[7] M. Carrasco, L. Pizarro, and D. Mery. Visual inspection of glass bottlenecks by multiple-view analysis. International Journal of Computer Integrated Manufacturing, 23(10):925–941, 2010.

[8] Z. Chen, Y. Zheng, B. R. Abidi, D. L. Page, and M. A. Abidi. A combinational approach to the fusion, denoising and enhancement of dual-energy X-ray luggage images. In IEEE Conference on Computer Vision and Pattern Recognition (CVPR-2005).

[9] N. Dalal and B. Triggs. Histograms of oriented gradients for human detection. In European Conference on Computer Vision (ECCV), 2005.

[10] J. Ding, Y. Li, X. Xu, and L. Wang. X-ray image segmentation by attribute relational graph matching. In 8th IEEE International Conference on Signal Processing, volume 2, 2006.

[11] X. Duan, J. Cheng, L. Zhang, Y. Xing, Z. Chen, and Z. Zhao. X-ray cargo container inspection system with few-view projection imaging. Nuclear Instruments and Methods in Physics Research A, 598:439–444, 2009.

[12] R. Duda, P. Hart, and D. Stork. Pattern Classification. John Wiley & Sons, Inc., New York, 2 edition, 2001.

[13] R. Eshel and Y. Moses. Tracking in a dense crowd using multiple cameras. International Journal of Computer Vision, 88:129–43, 2010.

[14] T. Franzel, U. Schmidt, and S. Roth. Object detection in multi-view X-ray images. Pattern Recognition, pages 144–154, 2012.

[15] I. Frosio, N. Borghese, F. Lissandrello, G. Venturino, and G. Rotondo. Optimized acquisition geometry for X-ray inspection. In Instrumentation and Measurement Technology Conference (I2MTC), 2011 IEEE, pages 1–6, 2011.

[16] J. Goebbels. Handbook of Technical Diagnostics, chapter Computed Tomography, pages 249–258. Springer, 2013.

[17] R. Gonzalez and R. Woods. Digital Image Processing, 2nd ed. Addison-Wesley, third edition, 2007.

[18] R. Haff and D. Slaughter. Real-time X-ray inspection of wheat for infestation by the granary weevil, sitophilus granarius (l.). Transactions of the American Society of Agricultural Engineers, 47:531–537, 2004.

[19] R. P. Haff and N. Toyofuku. X-ray detection of defects and contaminants in the food industry. Sensing and Instrumentation for Food Quality and Safety, 2(4):262–273, 2008.

[20] R. I. Hartley and A. Zisserman. Multiple view geometry in computer vision. Cambridge University Press, second edition, 2003.

[21] G. Heitz and G. Chechik. Object separation in X-ray image sets. In IEEE Conference on Computer Vision and Pattern Recognition (CVPR-2010), pages 2093–2100, 2010.

[22] C. Hellier. Handbook of Nondestructive Evaluation. McGraw Hill, second edition, 2013.

[23] J. Hubbell and S. Seltzer. Tables of X-Ray mass attenuation coefficients and mass energy-absorption coefficients from 1 keV to 20 MeV for elements Z = 1 to 92 and 48 additional substances of dosimetric interest. 1996
http://www.nist.gov/pml/data/xraycoef/index.cfm

[24] J.-A. Jiang, H.-Y. Chang, K.-H. Wu, C.-S. Ouyang, M.-M. Yang, E.-C. Yang, T.-W.Chen, and T.-T. L. a. An adaptive image segmentation algorithm for x-ray quarantine inspection of selected fruits. Computers and Electronics in Agriculture, 60:190–200, 2008.

[25] K. Konolige and M. Agrawal. FrameSLAM: from bundle adjustment to realtime visual mapping. IEEE Transactions on Robotics, 24(5):1066–1077, 2008.

[26] J.-S. Kwon, J.-M. Lee, and W.-Y. Kim. Real-time detection of foreign objects using x-ray imaging for dry food manufacturing line. In Proceedings of IEEE International Symposium on Consumer Electronics (ISCE 2008), pages 1–4, April 2008.

[27] X. Li, S. K. Tso, , X.-P. Guan, and Q. Huang. Improving automatic detection of defects in castings by applying wavelet technique. IEEE Transactions on Industrial Electronics, 53(6):1927–1934, 2006.

[28] T. Liao. Classification of weld flaws with imbalanced class data. Expert Systems with Applications, 35(3):1041–1052, 2008.

[29] T. Liao. Improving the accuracy of computer-aided radiographic weld inspection by feature selection. NDT&E International, 42:229-239, 2009.

[30] D. Lowe. Distinctive image features from scale-invariant keypoints. International Journal of Computer Vision, 60(2):91–110, 2004.

[31] Q. Lu and R. Conners. Using image processing methods to improve the explosive detection accuracy. IEEE Transactions on Applications and Reviews , Part C: Systems, Man, and Cybernetics, 36(6):750–760, 2006.

[32] M. Mansoor and R. Rajashankari. Detection of concealed weapons in X-ray images using fuzzy K-NN. International Journal of Computer Science, Engineering and Information Technology, 2(2), 2012.

[33] D. Mery. Explicit geometric model of a radioscopic imaging system. NDT & E International, 36(8):587–599, 2003.

[34] D. Mery. Exploiting multiple view geometry in X-ray testing: Part I, theory. Materials Evaluation, 61(11):1226–1233, November 2003.

[35] D. Mery. Automated radioscopic testing of aluminum die castings. Materials Evaluation, 64(2):135–143, 2006.

[36] D. Mery. Automated detection in complex objects using a tracking algorithm in multiple X-ray views. In Proceedings of the 8th IEEE Workshop on Object Tracking and Classification Beyond the Visible Spectrum (OTCBVS 2011), in Conjunction with CVPR 2011, Colorado Springs, pages 41–48, 2011.

[37] D. Mery. Automated detection of welding discontinuities without segmentation. Materials Evaluation, (June):657–663, 2011.

[38] D. Mery. X-ray testing by computer vision. In Proceedings of the 9th IEEE CVPR workshop on Perception Beyond the Visible Spectrum, Portland, 2013.

[39] D. Mery. X-ray testing: The state of the art. The e-Journal of Nondestructive Testing & Ultrasonics (www.ndt.net), 18(9), 2013.

[40] D. Mery and M. A. Berti. Automatic detection of welding defects using texture features. Insight-Non-Destructive Testing and Condition Monitoring, 45(10):676–681, 2003.

[41] D. Mery and D. Filbert. Automated flaw detection in aluminum castings based on the tracking of potential defects in a radioscopic image sequence. IEEE Trans. Robotics and Automation, 18(6):890–901, December 2002.

[42] D. Mery, I. Lillo, V. Riffo, A. Soto, A. Cipriano, and J. Aguilera. Automated fish bone detection using X-ray testing. Journal of Food Engineering, 2011(105):485–492, 2011.

[43] D. Mery, G. Mondragón, V. Riffo, , and I. Zuccar. Detection of regular objects in baggage using multiple x-ray views. Insight, 55(1):16–20, 2013.

[44] D. Mery, V. Riffo, I. Zuccar, and C. Pieringer. Automated X-ray object recognition using an efficient search algorithm in multiple views. In Proceedings of the 9th IEEE CVPR workshop on Perception Beyond the Visible Spectrum, Portland, 2013.

[45] D. Mery, U. Zscherpel, V. Riffo, G. Mondragón, I. Lillo, I. Zuccar, and H. Löbel. GDXray – the GRIMA database of X-ray images. Department of Computer Science, Universidad Católica de Chile. http://dmery.ing.puc.cl/index.php/material/gdxray/

[46] S. Michel, S. Koller, J. de Ruiter, R. Moerland, M. Hogervorst, and A. Schwaninger. Computer-based training increases efficiency in X-Ray image interpretation by aviation security screeners. pages 201–206, Oct. 2007.

[47] A. Noble, R. Gupta, J. Mundy, A. Schmitz, and R. Hartley. High precision X- ray stereo for automated 3D CAD-based inspection. IEEE Trans. Robotics and Automation, 14(2):292–302, 1998.

[48] Y. Ogawa, N. Kondo, and S. Shibusawa. Inside quality evaluation of fruit by x-ray image. volume 2, pages 1360–1365 vol.2, July 2003.

[49] C. Pieringer and D. Mery. Flaw detection in aluminium die castings using simultaneous combination of multiple views. Insight, 52(10):548–552, 2010.

[50] L. Pizarro, D. Mery, R. Delpiano, and M. Carrasco. Robust automated multiple view inspection. Pattern Analysis and Applications, 11(1):21–32, 2008.

[51] S. M. Rahman, M. O. Ahmad, and M. Swamy. Contrast-based fusion of noisy images using discrete wavelet transform. Image Processing, IET, 4(5):374–384, 2010.

[52] V. Riffo and D. Mery. Active X-ray testing of complex objects. Insight, 54(1):28–35, 2012.

[53] J. Rowlands. The physics of computed radiography. Physics in medicine and biology, 47(23):R123, 2002.

[54] L. Schmidt-Hackenberg, M. R. Yousefi, and T. M. Breuel. Visual cortex inspired features for object detection in X-ray images. In 21st International Conference on Pattern Recognition (ICPR), 2012, pages 2573–2576.

[55] D.-H. Shi, T. Gang, S.-Y. Yang, and Y. Yuan. Research on segmentation and distribution features of small defects in precision weldments with complex structure. NDT & E International, 40:397–404, 2007.

[56] R. Silva and D. Mery. State-of-the-art of weld seam inspection using X-ray testing: Part i image processing. Materials Evaluation, 65(6):643–647, 2007.

[57] R. Silva and D. Mery. State-of-the-art of weld seam inspection using X-ray testing: Part ii pattern recognition. Materials Evaluation, 65(9):833–838, 2007.

[58] M. Singh and S. Singh. Optimizing image enhancement for screening luggage at airports. In Computational Intelligence for Homeland Security and Personal Safety, 2005. CIHSPS 2005. Proceedings of the 2005 IEEE International Conference on, pages 131 –136, 31 2005-april 1 2005.

[59] S. Singh and M. Singh. Explosives detection systems (eds) for aviation security. Signal Processing, 83(1):31–55, 2003.

[60] H. Su, M. Sun, L. Fei-Fei, and S. Savarese. Learning a dense multi-view representation for detection, viewpoint classification and synthesis of object categories. In International Conference on Computer Vision (ICCV2009), 2009.

[61] Y. Tang, X. Zhang, X. Li, and X. Guan. Application of a new image segmentation method to detection of defects in castings. The International Journal of Advanced Manufacturing Technology, 43(5-6):431–439, 2009.

[62] J. Teubl and H. Bischof. Comparison of Multiple View Strategies to Reduce False Positives in Breast Imaging. Digital Mammography, pages 537–544, 2010.

[63] D. Turcsany, A. Mouton, and T. P. Breckon. Improving feature-based object recognition for X-ray baggage security screening using primed visualwords. In IEEE International Conference on Industrial Technology (ICIT), pages 1140–1145, 2013.

[64] R. Vilar, J. Zapata, and R. Ruiz. An automatic system of classification of weld defects in radiographic images. NDT & E International, 2009.

[65] P. Viola and M. Jones. Robust real-time object detection. International Journal of Computer Vision, 57(2):137–154, 2004.

[66] C. von Bastian, A. Schwaninger, and S. Michel. Do Multi-view X-ray Systems Improve X-ray Image Interpretation in Airport Security Screening?, volume 52. GRIN Verlag, 2010.

[67] Y. Wang, Y. Sun, P. Lv, and H. Wang. Detection of line weld defects based on multiple thresholds and support vector machine. NDT & E International, 41(7):517–524, 2008.

[68] K. Wells and D. Bradley. A review of X-ray explosives detection techniques for checked baggage. Applied Radiation and Isotopes, 2012.

[69] G. Zentai. X-ray imaging for homeland security. Imaging Systems and Techniques, 2008. IST 2008. IEEE International Workshop on, pages 1–6, Sept. 2008.

[70] Z. Zhu, Y.-C. Hu, and L. Zhao. Gamma/X-ray linear pushbroom stereo for 3D cargo inspection. Machine Vision and Applications, 21(4):413–425, 2010.

[71] Z. Zhu, L. Zhao, and J. Lei. 3d measurements in cargo inspection with a gamma-ray linear pushbroom stereo system. In Proceedings of the 2005 IEEE Computer Society Conference on Computer Vision and Pattern Recognition (CVPR05), 2005.

[72] V. Zografos, K. Nordberg, and L. Ellis. Sparse motion segmentation using multiple six-point consistencies. In Proceedings of the Asian Conference on Computer Vision (ACCV2010), 2010.